

# Fully Automated Extraction of Airways from CT Scans Based on Self-Adapting Region Growing

Oliver Weinheimer, Tobias Achenbach, and Christoph Düber

Department of Diagnostic and Interventional Radiology, Johannes Gutenberg  
University of Mainz, Germany  
mail@oliwe.com

**Abstract.** The segmentation of the airway tree is an important preliminary step for many clinical applications. In this paper we present a method for fully automated extraction of airways from volumetric computed tomography (CT) images based on a self-adapting region growing process. The method consists of 3 main steps. Firstly the histogram of a dataset is analysed. Secondly the trachea is searched and segmented. And thirdly the bronchial tree is segmented by a self-adapting region growing process. The proposed method has been applied to 40 patient datasets provided by EXACT09, a comparative study of airway extraction algorithms. Former versions of our method have been used extensively in many clinical studies.

## 1 Introduction

Computed tomography (CT) is currently the method of choice for noninvasive and sensitive imaging of pathologic changes in the lung. Development of multidetector CT (MDCT) combines the advantages of the high-resolution CT (HRCT) and spiral CT and allows visualisation of the lungs and the bronchial tree up to the subsegmental level. A fast and reliable extraction of the airway tree is of fundamental importance for many clinical applications like a noninvasive 3D measurement and quantification of airway geometry [1, 2], computer-assisted bronchoscopy [3] or emphysema quantification [4]. Many semi-automatic and automatic methods have been presented in the past for extracting the airway tree in volumetric CT scans, e.g. [5–8]. Low dose CT scans and ultra low dose scans are increasingly utilised in lung screening studies. Lowering the radiation exposure increases the amount of noise in the CT images, hence it increases the demands on fast and reliable airway extraction methods. So far, there have been no perfect extraction techniques, however events like EXACT09 are important for comparing and improving different airway extraction methods.

## 2 Fully Automated Extraction of Airways from CT

Depending on the quality of the data bronchial tree extraction can be a very challenging task - especially if it is a fully automated extraction. Our proposed

method in this paper is based on the method first introduced in [9]. We improved the procedure over time while using it for many studies, see e.g. [1, 4, 10–13]. The datasets of these studies were generated with a normal clinical dose - datasets of this quality were the main field of application of former versions of our method. The datasets provided by EXACT09 range from clinical dose to ultra low dose scans, from healthy volunteers to patients with severe lung disease, and from full inspiration to full expiration. All images had a matrix size of  $512 \times 512$ . We additionally integrated slight modifications to our existing method so that it was applicable to the challenging datasets of EXACT09. The method consists now of 3 main steps. Firstly the histogram of a dataset is analysed. Secondly the trachea is searched and segmented. Thirdly the bronchial tree is segmented by a self-adapting region growing process.

## 2.1 Step 1: Histogram Analysis

The fundamental importance of calibration for a CT system is indisputable. A CT system should be well calibrated, such that air is at -1000 HU, while water is at 0 HU. For this reason the first peak in the histogram of the first 10 upper slices of a dataset is determined and assigned to the variable  $T_{\text{Air}}$ . The peak value should be -1000 HU. After temporarily applying a Gaussian filter to these slices and recalculating the histogram, the first peak is assigned to the variable  $T'_{\text{Air}}$ . The Gaussian filter should not change the position of the first peak. We distinguish between two cases. Firstly, if  $T_{\text{Air}} \neq T'_{\text{Air}}$ , see e.g. Fig. 1(a)(b), the  $3 \times 3$  Gaussian mask  $\frac{1}{4} [1 \ 2 \ 1] * \frac{1}{4} [1 \ 2 \ 1]^T$  is applied to each slice of the whole dataset. The inequality is caused in this case by a CT system where the range of the CT numbers is limited by  $-1024$  HU and a hard reconstruction kernel was used, hence it is a sign of noise in the images. Secondly, if  $T_{\text{Air}} \neq -1000$  HU (see e.g. Fig. 1(c)(d)), the CT system is not well calibrated to air. The air calibration error will be dealt with in step 3.

## 2.2 Step 2: Searching for the Trachea

The trachea search is realised on the upper slices of a data set. A body detection is performed, so that the search area for the trachea can be limited to the body region. Then a circular region with voxel values  $< -500$  HU (dark region) is searched on the axial slices inside the detected body. The 2D region must be greater than  $5^2 \times \pi \text{ mm}^2$  and smaller than  $15^2 \times \pi \text{ mm}^2$ . The centre of gravity of the region is calculated and mapped on the succeeding slice. The mapped point should be part of a similar dark region, additionally the top of one lung is searched on this slice. If all conditions are fulfilled, a trachea landmark is found. If no Gaussian filter was applied to the dataset in step 1, the noise is quantified in the trachea region found and if necessary a  $3 \times 3$  Gaussian mask is applied to the whole dataset. The trachea is then segmented with a 2D region growing with threshold value  $-500$  HU, always mapping the centre of gravity of a marked region to the succeeding slice in basal direction as a new seed point. The procedure stops if the carina (main bifurcation of the trachea) is reached.

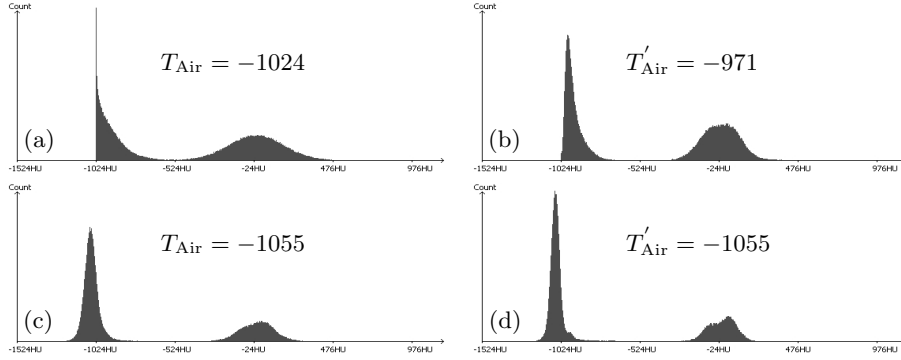


**Fig. 1.** (a) Histogram of CASE21 (Siemens Sensation 64, Kernel B50f, Pixel Spacing: 0.60 mm, Slice Thickness: 0.60 mm, Spacing Between Slices: 0.60 mm, Exposure: 100 mAs, 120 kVp). Values  $< -1024$  HU are mapped on  $-1024$  HU. Useful information is lost. (b) Histogram of CASE21 after applying a Gaussian filter.  $T'_{\text{Air}}$  is greater than  $-1000$  HU because of the lost information described in (a). (c) Histogram of CASE24 (Toshiba Aquilion, Kernel FC12, Pixel Spacing: 0.65 mm, Slice Thickness: 1.00 mm, Spacing Between Slices: 0.8 mm, Exposure: 5 mAs, 120 kVp). (d) Histogram of CASE24 after applying a Gaussian filter. The Gaussian filter did not change the position of the first peak. This dataset is not well calibrated, because  $T'_{\text{Air}} = T_{\text{Air}} = -1055$ . This indicates a calibration error of 55 HU.

### 2.3 Step 3: Self-Adapting Region Growing

Step 2 supplies a starting voxel within the trachea for an iterative, self-adapting and region growing based 3D bronchial tree tracer. This starting voxel is marked as “bronchusL” (L for large). All connected voxels are written in a queue. 3D region growing with a  $N_{26}$  neighbourhood system is started for all voxels added to the queue, starting with the first one. We define  $T_{\text{Lumen},i,i=0} = -950 + (T_{\text{Air}} + 1000)$  and  $T_{\text{Wall},i,i=0} = T_{\text{Lumen}} + 175$  for the first iteration. A voxel is marked as “bronchusL” if the mean value in  $N_7$  neighbourhood  $< T_{\text{Lumen},i}$ , the maximal value in  $N_{27} < T_{\text{Wall},i}$  and the voxel is connected to another voxel marked as “bronchusL”. The conditions are selected so restrictively that leaking out of the segmentation into the lung parenchyma is almost impossible. If the conditions are not fulfilled, it is examined whether a voxel is in a smaller bronchus. The rationale for the 2nd evaluation is the following: a bronchus will be cut either by a axial, coronal or sagittal plane in a circular to elliptical way. If a voxel lies within a bronchus, then it is surrounded by bronchial wall in one of the planes in all directions. The algorithm does not examine all directions, but in each plane 8 rays as direction of detection are cast outwards. On each ray the maximal positive gradient and the maximal HU value are determined. Then it is determined if a voxel is air and if it is surrounded by airway wall in one plane in all directions. The evaluation is based on fuzzy logic rules, which takes into account the average HU value, the maximal positive gradient and the maximal HU value on the rays. Again the conditions are selected so restrictively that “leaking out”

into the lung parenchyma is almost impossible. If a voxel is identified as lumen voxel in one plane, the voxel is marked according to the plane in which it has been identified as “bronchusS” (sagittal), “bronchusC” (coronal) or “bronchusA” (axial). If more than a defined permitted number of voxels are added by a single region growing process, the marked voxels are reset to unmarked in order to avoid leaking out into lung parenchyma. If all voxels in the queue are processed,  $T_{\text{Lumen}_{i+1}} = T_{\text{Lumen}_i} + \Delta T$  is set for the next iteration. All unmarked voxels, connected to the detected bronchial tree so far, are written in a queue and region growing starts again for all voxels added to the queue. The method stops if  $T_{\text{Lumen}_{i+1}} > T_{\text{Lumen}_0} + \Delta T_{\text{max}}$  or leakage occurred more than  $L_{\text{max}}$  times. We use  $\Delta T_{\text{max}} = 100$ ,  $\Delta T = 1$  and  $L_{\text{max}} = 5$  by default.

After finalisation of step 3, holes in the segmented bronchial tree are closed.

### 3 Results and Discussion

The images used in this challenge were volumetric chest CT scans acquired at different sites using several different scanners, scanning protocols, and reconstruction parameters. The images were divided into two sets: a training set (CASE01-CASE20) and a testing set (CASE21-CASE40). We used the training set in order to slightly modify our existing method so that it was able to cope with the EXACT data. The datasets range from clinical dose to ultra low dose scans, from healthy volunteers to patients with severe lung disease, and from full inspiration to full expiration. Our proposed method was able to extract the bronchial tree fully automatic in all 40 datasets. We submitted our segmentation results to EXACT09. The segmentations of the 15 participating teams were centrally evaluated by a team of trained observers. For this purpose, a ground truth was constructed from all submitted segmentations and all submissions were subsequently evaluated with respect to this ground truth. For details on the set-up of the study, collection of data and evaluation of segmentations, acquisition parameters of the 20 test cases, and the seven evaluation measures computed see [14]. Table 1 documents the results achieved with our method for the 20 cases in the testing set. An average number of 130.1 branches were detected in the datasets (mean value for all teams: 124.01). The mean value for the leakage volume was 559.0 mm<sup>3</sup> (mean value for all teams: 700.55 mm<sup>3</sup>). In 10 cases no leakage occurred - in 10 cases leakage occurred. Fig. 2(a) shows CASE32, where the greatest leakage volume was measured. Fig. 2(b) shows CASE22, where the greatest number of branches were determined. The average runtime on a PC (Intel Xeon CPU, 2.83 GHz, 4GB RAM) per case of the testing set was 183 s, 39 s for Step 1 and 2 and 144 s for Step 3.

Our implemented leakage detection is just based on the number of added voxels by a single region growing process - this simple rule should be improved, shape features can be used for this purpose. It should be possible with an improved leakage detection to increase the upper Hounsfield limit, specified by  $\Delta T_{\text{max}}$ , in step 3 of the method. This should allow the segmentation of more peripheral bronchi. The rules for the detection of smaller airways in step 3 should

**Table 1.** Evaluation measures for the 20 cases in the test set.

	Branch count	Branch detected (%)	Tree length (cm)	Tree length detected (%)	Leakage count	Leakage volume (mm <sup>3</sup> )	False positive rate (%)
CASE21	103	51.8	54.7	49.5	3	651.4	6.93
CASE22	252	65.1	181.3	54.9	2	8.9	0.04
CASE23	154	54.2	100.6	38.7	0	0.0	0.00
CASE24	101	54.3	76.0	46.7	0	0.0	0.00
CASE25	134	57.3	100.7	40.0	0	0.0	0.00
CASE26	39	48.8	28.8	43.8	0	0.0	0.00
CASE27	34	33.7	25.0	30.8	0	0.0	0.00
CASE28	98	79.7	71.6	65.3	7	214.3	1.69
CASE29	111	60.3	69.8	50.6	5	131.3	1.04
CASE30	144	73.8	108.8	71.2	12	2226.0	12.37
CASE31	173	80.8	134.2	76.5	21	1956.2	7.38
CASE32	155	66.5	130.6	60.0	20	3563.2	10.79
CASE33	119	70.8	87.2	59.3	1	15.3	0.15
CASE34	251	54.8	158.6	44.3	0	0.0	0.00
CASE35	104	30.2	64.9	21.0	0	0.0	0.00
CASE36	129	35.4	135.1	32.8	0	0.0	0.00
CASE37	52	28.1	44.8	25.2	0	0.0	0.00
CASE38	35	35.7	27.7	41.7	0	0.0	0.00
CASE39	176	33.8	129.3	31.6	12	461.3	3.51
CASE40	238	61.2	187.0	48.3	29	1952.7	5.46
Mean	130.1	53.8	95.8	46.6	5.6	559.0	2.47
Std. dev.	66.1	16.6	49.3	14.9	8.7	1019.3	3.95
Min	34	28.1	25.0	21.0	0	0.0	0.00
1st quartile	98	35.4	54.7	32.8	0	0.0	0.00
Median	124	54.6	93.9	45.5	1	4.5	0.02
3rd quartile	176	70.8	135.1	60.0	12	1952.7	6.93
Max	252	80.8	187.0	76.5	29	3563.2	12.37

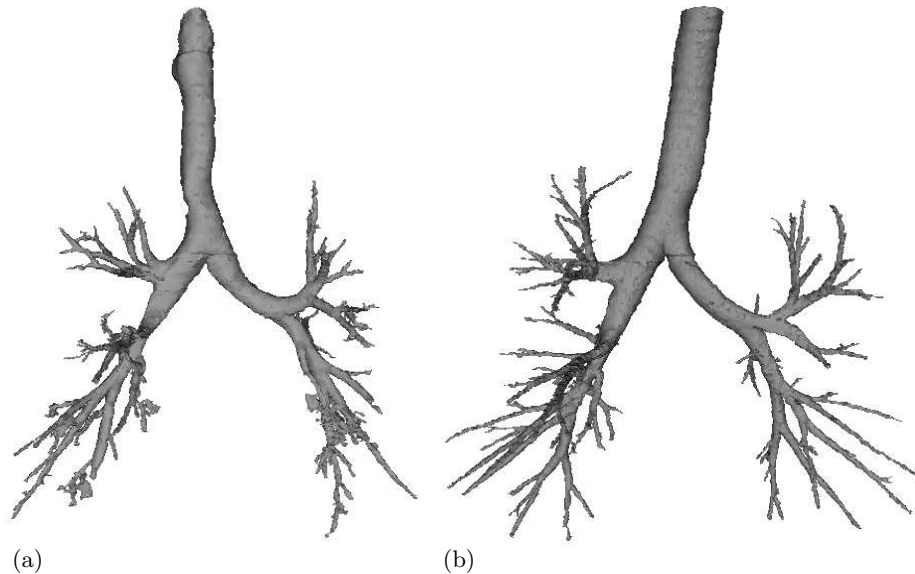


**Fig. 2.** Two segmented bronchial trees rendered with the marching cubes algorithm. (a) CASE32 (Philips Mx8000 IDT 16, D Kernel, Pixel Spacing: 0.78 mm, Slice Thickness: 1.0 mm, Spacing Between Slices: 1.0 mm, Exposure: 40 mAs, 140 kVp). Dataset with the greatest value for leakage volume ( $3563.2 \text{ mm}^3$ ). (b) CASE22 (Siemens Sensation 64, B50f Kernel, Pixel Spacing: 0.60 mm, Slice Thickness: 0.6 mm, Spacing Between Slices: 0.6 mm, Exposure: 100 mAs, 120 kVp). Dataset with the greatest value for branch count, 253 branches were detected, leakage volume =  $8.9 \text{ mm}^3$ .

be reworked and additionally more than the 3 main cutting planes (axial, sagittal, coronal) should be used for the decision-making process. Furthermore, 2D airway detection should be applied to a dataset and the results connected to the 3D segmentation. This can help to detect airway stenosis.

In this paper we presented a method for fully automated extraction of airways from CT Scans. Our method worked well on the challenging datasets of EXACT09, nevertheless we have gathered valuable information for our future work. Generating a common database covering a wide range of possible CT scans is an important step for improving and comparing different airway extraction methods.

## References

1. Achenbach, T., Weinheimer, O., Biedermann, A., Schmitt, S., Freudenstein, D., Gouthma, E., Kunz, R.P., Buhl, R., Dueber, C., Heußel, C.P.: MDCT Assessment of Airway Wall Thickness in COPD Patients Using a New Method: Correlations with Pulmonary Function Tests. *European Radiology* **18** (2008) 2731–2738

2. Saba, O.I., Hoffman, E.A., Reinhardt, J.M.: Maximizing Quantitative Accuracy of Lung Airway Lumen and Wall Measures Obtained from X-Ray CT Imaging. *Journal of Applied Physiology* **95** (2003) 1063–1075
3. Kiraly, A.P., Helferty, J.P., Hoffman, E.A., McLennan, G., Higgins, W.E.: Three-Dimensional Path Planning for Virtual Bronchoscopy. *IEEE Trans. Med. Imaging* **23**(9) (2004) 1365–1379
4. Heußel, C.P., Herth, F., Kappes, J., Hantusch, R., Hartlieb, S., Weinheimer, O., Kauczor, H.U., Eberhardt, R.: Fully-Automatic Quantitative Assessment of Emphysema in Computed Tomography – Comparison with Pulmonary Function Testing and Normal Values. *European Radiology* (2009)
5. van Ginneken, B., Baggerman, W., Rikxoort, E.M.: Robust Segmentation and Anatomical Labeling of the Airway Tree from Thoracic CT Scans. In: MICCAI 2008. Volume LNCS 5241.
6. Tschirren, J., Hoffman, E.A., McLennan, G., Sonka, M.: Intrathoracic Airway Trees: Segmentation and Airway Morphology Analysis from Low-Dose CT Scans. *IEEE Trans. Med. Imaging* **24**(12) (2005) 1529–1539
7. Fetita, C., Prêteux, F., Beigelman-Aubry, C., Grenier, P.: Pulmonary Airways: 3-D Reconstruction From Multislice CT and Clinical Investigation. *IEEE Trans. Med. Imaging* **23**(11) (2004) 1353–1364
8. Kiraly, A.P., Higgins, W.E., McLennan, G., Hoffman, E.A., Reinhardt, J.M.: Three-dimensional Human Airway Segmentation Methods for Clinical Virtual Bronchoscopy. *Academic Radiology* **9**(10) (2002) 1153–1168
9. Weinheimer, O., Achenbach, T., Buschsieweke, C., Heußel, C.P., Uthmann, T., Kauczor, H.U.: Quantification and Characterization of Pulmonary Emphysema in Multislice-CT: A Fully Automated Approach. In Petra Perner, Rüdiger W. Brause and Hermann-Georg Holzhütter, eds.: *Medical Data Analysis, 4th International Symposium, ISMDA 2003, Berlin, Germany, October 9-10, 2003, Proceedings*. Volume 2868 of *Lecture Notes in Computer Science*. Springer (2003)
10. Heußel, C.P., Kappes, J., Hantusch, R., Hartlieb, S., Weinheimer, O., Kauczor, H.U., Eberhardt, R.: Contrast Enhanced CT-Scans are not Comparable to Non-Enhanced Scans in Emphysema Quantification. *European Journal of Radiology* (accepted) (2009)
11. Weinheimer, O., Achenbach, T., Bletz, C., Düber, C., Kauczor, H.U., Heußel, C.P.: About Objective 3-D Analysis of Airway Geometry in Computerized Tomography. *IEEE Trans. Med. Imaging* **27**(1) (2008) 64–74
12. Heußel, C.P., Achenbach, T., Buschsieweke, C., Kuhnigk, J., Weinheimer, O., Hammer, G., Düber, C., Kauczor, H.U.: Quantifizierung des Lungenemphysems in der Mehrschicht-CT mittels verschiedener Softwareverfahren: Quantification of Pulmonary Emphysema in Multislice-CT Using Different Software Tools. *Fortschr Röntgenstr (Röfo)* **178** (2006) 987–998
13. Zaporozhan, J., Ley, S., Eberhardt, R., Weinheimer, O., Iliyushenko, S., Herth, F., Kauczor, H.U.: Paired Inspiratory/Expiratory Volumetric Thin-Slice CT Scan for Emphysema Analysis: Comparison of Different Quantitative Evaluations and Pulmonary Function Test. *Chest* **128** (2005) 3212–3220
14. Lo, P., van Ginneken, B., Reinhardt, J., de Bruijne, M.: Extraction of Airways from CT (EXACT’09). In: *Second International Workshop on Pulmonary Image Analysis*. (2009)